

Priority Report

Real-time Monitoring of *In Vivo* Acute Necrotic Cancer Cell Death Induced by Near Infrared Photoimmunotherapy Using Fluorescence Lifetime Imaging

Takahito Nakajima, Kohei Sano, Makoto Mitsunaga, Peter L. Choyke, and Hisataka Kobayashi

Abstract

A new type of monoclonal antibody (mAb)-based, highly specific phototherapy (photoimmunotherapy; PIT) that uses a near infrared (NIR) phthalocyanine dye, IRDye700DX (IR700) conjugated with a mAb, has recently been described. NIR light exposure leads to immediate, target-selective necrotic cell death *in vitro*. Detecting immediate *in vivo* cell death is more difficult because it takes at least 3 days for the tumor to begin to shrink in size. In this study, fluorescence lifetime (FLT) was evaluated before and after PIT for monitoring the immediate cytotoxic effects of NIR mediated mAb-IR700 PIT. Anti-epidermal growth factor receptor (EGFR) panitumumab-IR700 was used for targeting EGFR-expressing A431 tumor cells. PIT with various doses of NIR light was conducted in cell pellets *in vitro* and in subcutaneously xenografted tumors in mice *in vivo*. FLT measurements were obtained before and 0, 6, 24, and 48 hours after PIT. *In vitro*, PIT at higher doses of NIR light immediately led to FLT shortening in A431 cells. *In vivo* PIT induced immediate shortening of FLT in treated tumors after a threshold NIR dose of 30 J/cm² or greater. In contrast, lower levels of NIR light (10 J/cm² or smaller) did not induce shortening of FLT. Prolongation of FLT in tissue surrounding the tumor site was noted 6 hours after PIT, likely reflecting phagocytosis by macrophages. In conclusion, FLT imaging can be used to monitor the acute cytotoxic effects of mAb-IR700-induced PIT even before morphological changes can be seen in the targeted tumors. *Cancer Res*; 72(18); 4622–8. ©2012 AACR.

Introduction

Most of the side effects of current cancer therapies are caused by damage to normal cells. Therefore, maximizing cytotoxicity to cancer cells while minimizing damage to normal cells is a highly desirable design criterion for new therapies. We recently developed a new type of monoclonal antibody (mAb)-based, highly specific phototherapy (photoimmunotherapy; PIT) that uses a near infrared (NIR) phthalocyanine dye, IRDye700DX (IR700) conjugated with mAb (1, 2). When the mAb-IR700 conjugate binds to the target cell and is exposed to sufficient, but still nonthermal, doses of NIR light, highly specific and immediate cell death occurs. The therapeutic effect is only observed if the mAb-IR700 binds to the target cell membrane and is exposed to NIR, otherwise the conjugate is harmless to nontargeted cells. Although targeted cell death can be observed immediately *in vitro* it is more challenging to see immediate changes *in vivo* because size changes take 3 to 4 days to become visible (3). Real-time monitoring of PIT effects could be important for ascertaining whether a PIT session has

been effective and whether additional cycles of therapy are needed (1). This might include additional doses of light, higher intensity light or additional doses of the mAb-IR700 conjugate or all of these. Immediate feedback is especially important during surgical or interventional procedures under endoscopy. However, no clinically applicable imaging technology exists for assessing real-time effects of PIT (4, 5).

In addition to being a potent photosensitizer, IR700 is also a fluorophore. Its fluorescence can be used to direct NIR light, thus further reducing potential toxicity. IR700 has a relatively long fluorescence lifetime (FLT; refs. 6–12), and therefore, a change in IR700 FLT could be a good predictor of target cell death. In this study, we measured the FLT of mAb-IR700 after PIT with various doses of NIR light exposure and used FLT for real-time monitoring of the cytotoxic effects of PIT.

Materials and Methods**Reagents**

Panitumumab, a fully humanized IgG2 mAb directed against the human epidermal growth factor receptor (EGFR), or HER1, was purchased from AMGEN Inc. A water soluble, silicon-phthalocyanine derivative, IRDye 700DX NHS ester (IR700; C₇₄H₉₆N₁₂Na₄O₂₇S₆Si₃, molecular weight of 1954.22) was purchased from LI-COR Bioscience. All other chemicals used were of reagent grade.

Synthesis of IR700-conjugated panitumumab

Panitumumab (1 mg, 6.8 nmol) was incubated with IR700 (66.8 μg, 34.2 nmol, 5 mmol/L in DMSO) in 0.1 mol/L Na₂

Authors' Affiliation: Molecular Imaging Program, Center for Cancer Research, National Cancer Institute, National Institutes of Health, Bethesda, Maryland.

Corresponding Author: Hisataka Kobayashi, Molecular Imaging Program, Center for Cancer Research, National Cancer Institute, NIH, Building 10, Room B3B69, MSC1088, Bethesda, MD 20892. Phone: 301-451-4220; Fax: 301-402-3191; E-mail: kobayash@mail.nih.gov

doi: 10.1158/0008-5472.CAN-12-1298

©2012 American Association for Cancer Research.

HPO₄ (pH 8.6) at room temperature for 1 hour. Then the mixture was purified with a Sephadex G50 column (PD-10; GE Healthcare). The protein concentrations were determined with Coomassie Plus Protein Assay Kit (Pierce Biotechnology) by measuring light absorption at 595 nm (8453 Value System; Agilent Technologies). The concentration of IR700 was measured by absorption with spectroscopy to confirm the average number of fluorophore molecules conjugated to each panitumumab molecule. The number of IR700 per antibody was approximately 4 for the 1:4.5 reaction conditions. The addition of 0.4% SDS to the sample dissociated the fluorophores from each other, effectively causing dequenching. Quenching efficiency for a particular conjugation is defined as the fluorescence intensity with SDS divided by fluorescence intensity without SDS. Panitumumab-IR700 conjugate (Pan-IR700) showed a quenching efficiency of about 4.0 at pH 7.2. Pan-IR700 was kept at 4°C in the refrigerator as a stock solution.

Fluorescence lifetime measurements

All FLT experiments were conducted with the eXplore Optix-MX2 system (ART Advanced Research Technologies, Inc.; refs. 13, 14). A fixed pulsed laser diode was used as an excitation source at a wavelength of 670 nm. Region of interest (ROI) measurements with a spot size of 1.5 mm were selected at the image plane. The laser power was automatically chosen as the highest power that does not saturate the photon detector.

Lifetime analysis was conducted by using the ART OptiView (ART Advanced Research Technologies, Inc.). Lifetime values and lifetime mapping were calculated to fit fluorescence temporal point-spread functions (TPSFs) as single-exponential models with the Fit TPSF tool.

PIT for *in vitro* and *in vivo* models

PIT was conducted with a red light-emitting diode (LED) light at 680 to 700 nm wavelength (Tech-LED, Marubeni America Co.; ref. 2). Power densities were measured with an optical power meter (PM 100, Thorlabs).

Determination of FLT for Pan-IR700

Samples of Pan-IR700 at concentrations of 2.5, 5, 20, and 40 µg/mL were prepared by dilution with PBS. The fluorescence intensities and lifetimes of each sample were determined using the Optix MX2 system at room temperature within a 1.7 mL centrifuge tube.

To investigate the effect of PIT using Pan-IR700, the FLT of each sample at the concentration of 50 µg/mL was measured after irradiating the samples at a PIT dose of 0, 2, 4, 8, 15, and 30 J/cm².

Cell line

The HER1 positive cell line, A431 was used for HER1 targeting studies with panitumumab conjugates. The cell line was grown in RPMI 1640 (Life Technologies) containing 10% fetal bovine serum (Life Technologies), 0.03% L-glutamine, 100 units/mL penicillin, and 100 µg/mL streptomycin in 5% CO₂ at 37°C.

Cell pellet FLT studies

A431 cells were plated on 75 mm² cell culture flasks and incubated until confluent. Then Pan-IR700 conjugate was added to the media (1 µg/mL), and cells were incubated for 24 hours at 37°C. Upon completion of incubation, cells were removed from the flasks, and centrifuged to obtain pellets. The resulting cell pellets were washed three times with PBS and placed in 1.7 mL centrifuge tubes. The fluorescence intensities and lifetimes of each sample were then obtained.

To investigate the effect of cellular internalization with Pan-IR700 conjugates, A431 cells were plated on a 75 mm² flask and were incubated with Pan-IR700 for 1, 2, 4, 6, 15, and 24 hours. After removing the flasks and obtaining A431 cell pellets, FLT measurements of the A431 pellet was acquired.

After the A431 cell pellets were incubated overnight with Pan-IR700, cell pellets were irradiated at doses of 0, 2, 4, 8, 15, and 30 J/cm². After that, these pellets were gently washed with PBS × 1 and fluorescence intensity and lifetime images were obtained.

To detect the antigen specific localization of IR700 and to confirm the morphologic changes of A431 cells before and after PIT, fluorescence microscopy was conducted using Olympus BX61 microscope (Olympus America) equipped with the following filters: a 590 to 650 nm excitation filter, a 665 to 740 nm band pass emission filter. Transmitted light differential interference contrast images were also acquired. A431 cells were plated on a cover glass-bottomed culture well and incubated for 24 hours. Pan-IR700 was added to the medium (10 µg/mL), and the cells were incubated for either 6 or 24 hours. Once complete, the cells were washed once with PBS, and fluorescence microscopy was conducted before and after PIT.

Mouse model

All procedures were carried out in compliance with the Guide for the Care and Use of Laboratory Animal Resources (1996), National Research Council, and approved by the local Animal Care and Use Committee. A431 cells (1 × 10⁶ cells) were injected subcutaneously on both sides of the dorsum of female nude mice (National Cancer Institute Animal Production Facility). The experiments were conducted at 6 to 9 days after cell injection.

In vivo FLT imaging studies after PIT

Tumor-bearing mice were divided into 3 groups of 5 mice per group for the following irradiation doses of PIT: 10, 30, and 50 J/cm². As a control, 5 mice were prepared without PIT. One hundred micrograms of Pan-IR700 were injected intravenously via the tail vein into every mouse 24 hours before PIT. A431 tumors in the right-hand side of the dorsum were treated with PIT while the contralateral control tumors were shielded from light exposure with aluminum foil. After PIT, FLT images were obtained at the following time points: 0, 6, 24, and 48 hours. Zero hours acquisitions were conducted immediately after PIT. Maximum spot values of each ROI in the FLT images were calculated for tumors on both sides of the dorsum.

Histologic analysis

To evaluate serial histologic changes immediately (within 5 minutes) after PIT with various NIR light doses, microscopy was conducted (BX51, Olympus America). A431 tumors were harvested in 10% formalin immediately after 0, 10, 30, and 50 J/cm² of NIR light exposure. Serial 10- μ m slice sections were fixed on a glass slide with H&E staining.

Statistical analysis

Statistical analyses were carried out using a statistics program (GraphPad Prism; GraphPad Software). Mann-Whitney's *U* test was used to compare the lifetime value between those of treated tumors and untreated tumors. Student *t* test was used to compare with the lifetimes of treated tumors to no treatment control. *P* < 0.05 was considered to indicate a statistically significant difference.

Results

FLT is independent from the Pan-IR700 concentration in the solution

The FLTs of various concentrations of Pan-IR700 were approximately the same, 3.56 \pm 0.08 nanoseconds (ns); 3.62 (2.5 μ g/mL), 3.58 (5 μ g/mL), 3.44 (20 μ g/mL), 3.60 ns (40 μ g/mL),

whereas the fluorescence intensities were decreased in proportion to the concentration (Fig. 1A and B).

NIR light exposure alone does not affect the FLT of Pan-IR700

Pan-IR700 (50 μ g/mL) by itself was irradiated and FLT was measured. Both fluorescence intensity and lifetime did not change by irradiation of LED at the dose of 0, 2, 4, 8, 15, and 30 J/cm². The FLT was approximately 3.44 \pm 0.06 ns.

Internalization of Pan-IR700 prolonged the IR700 FLT

FLT of A431 cells increased with the duration of the incubation with Pan-IR700. The FLTs of A431 cell pellet at 1, 2, 4, 6, 15, and 24 hours of incubation were 2.98, 3.05, 3.13, 3.15, 3.36, and 3.41 ns, respectively. After 15 hours incubation, FLT of IR700 reached its peak and showed no further prolongation (Fig. 1D).

Greater exposure of NIR light shortened the FLT of IR700 containing A431 cells

PIT with greater NIR light doses induced greater shortening of FLT in A431 cell pellets incubated with Pan-IR700 for 24 hours before exposure to the NIR light (Fig. 1C). PIT shortened

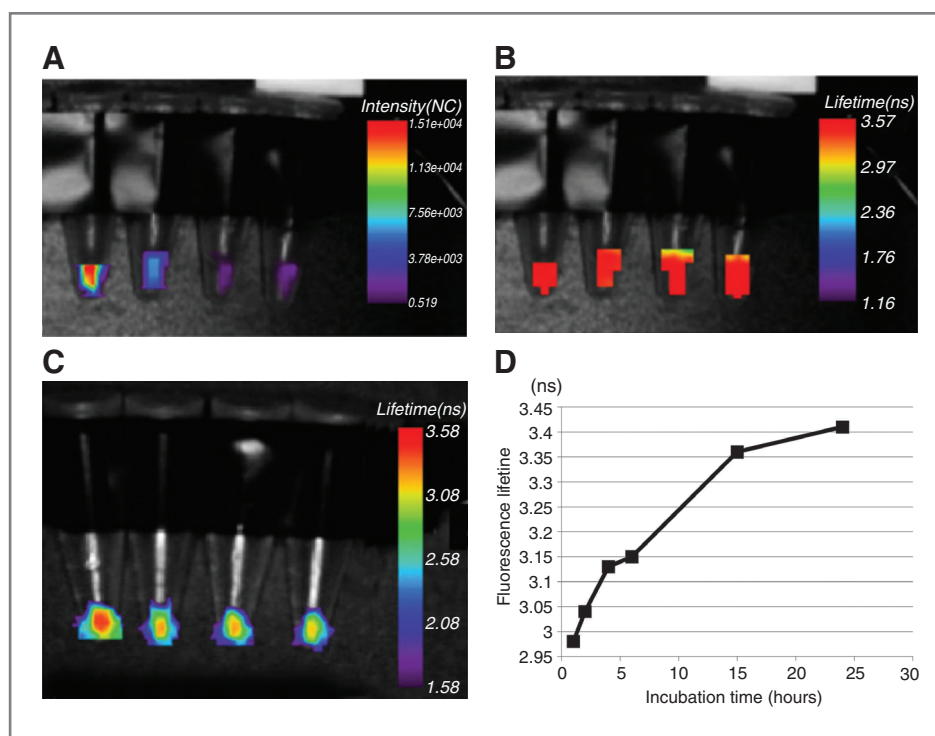


Figure 1. Samples of IR700-conjugated panitumumab (Pan-IR700) at concentrations of 2.5, 5, 20, and 40 μ g/mL were prepared by diluting with PBS. A, fluorescence intensity image of Pan-IR700 solution. Fluorescence intensities were decreased according to decrease of concentration of Pan-IR700. B, fluorescence lifetime (FLT) image of Pan-IR700 solution. The FLT at various concentrations of Pan-IR700 solutions was almost the same value, 3.56 \pm 0.081 nanoseconds (ns); 3.62 (2.5 μ g/mL), 3.58 (5 μ g/mL), 3.44 (20 μ g/mL), 3.60 ns (40 μ g/mL). C, LED light-irradiation for A431 cell pellets changes FLTs. A431 cell line incubated with Pan-IR700 for 24 hours were treated with PIT at doses of 0, 8, 15, and 30 J/cm². FLT shortened to 3.09, 2.94, and 2.85 ns, compared with 3.28 ns before light exposure. These represented shortenings of 9.1%, 10.1%, and 13.1%, respectively. D, FLT of A431 pellets depends on the incubation time with Pan-IR700. FLT values escalate with incubation time with Pan-IR700. FLT changes from 2.98 ns (1 hour) to 3.42 ns (24 hours).

the FLT of A431 pellets down to 3.28, 3.09, 2.94, and 2.85 ns at doses of 0, 8, 15, and 30 J/cm², respectively.

PIT induced typical necrotic cell death in A431 cells as well as rupture of lysosomes

Under microscopy, Pan-IR700 was seen on the cell membrane and within endolysosomes at 24 hours after incubation. Following exposure to NIR light, immediate damage was induced in the cell membranes and lysosomes. Multifocal bleb formation was seen in the cellular membranes, characteristic of necrotic cell death induced by PIT (Fig. 2).

Effective PIT induced immediate shortening of the FLT of IR700 *in vivo*

The average FLT of A431 tumors 1 day after administration of 100 µg of Pan-IR700 *in vivo* was 3.27 ± 0.46 ns (*n* = 40). Significant shortening of FLT was induced immediately after PIT with NIR light doses of 30 and 50 J/cm² to experimental tumors (right dorsum, 30 J/cm²; down to 61.5% ± 5.1% of untreated tumors in the same mouse; *P* < 0.01, 50 J/cm²; down to 69.0% ± 10.9% of untreated tumors in the same mouse; *P* < 0.05).

Transient prolongation of IR700 FLT was found in and around PIT treated tumors 6 hours after PIT at NIR light doses of 30 and 50 J/cm² but continued to shorten at ≥24 hours after PIT. PIT with 10 J/cm² did not show this transiently prolonged FLT. IR700 FLT in untreated control tumors also slightly shortened at late time points (Fig. 3A).

Comparison with IR700 FLT between exposed and nonexposed tumors with NIR light of 30 and 50 J/cm² in the same mice showed significant differences within 5 minutes and, 24

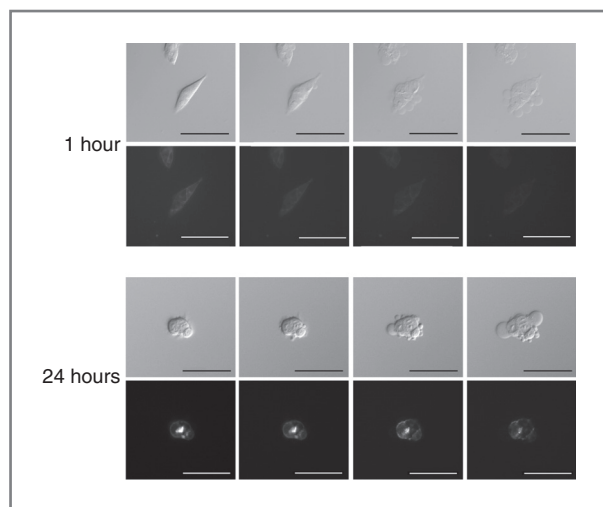


Figure 2. Serial fluorescence (bottom) and differential interference contrast microscopic images (top) of A431 cells, which were preincubated with Pan-IR700 (10 µg/mL) at 37°C for 24 hours, 5, 15, 60, and 90 seconds after start of exposing NIR light. (Pan-IR700 gradually internalized into cytoplasm in A431 cells after bound to cell membrane up to 24 hours after starting incubation.) Morphologic changes in differential interference contrast become severer with exposure to increased dose of NIR light. Scale bars, 50 µm.

and 48 hours after PIT (*P* < 0.05; Fig. 3B and C). The differences of IR700 FLT at 6 hours post-PIT were not statistically significant due to the diffuse temporal increase around exposed tumors. IR700 FLT of exposed and nonexposed tumors with NIR light of 10 J/cm² did not show significant difference at any time point (Fig. 3D).

FLT in PIT treated tumors with 50 and 30 J/cm² shortened significantly (*P* < 0.01) compared with no treatment controls (0 J/cm²). FLTs were immediately shortened to 69.1% ± 10.9% and 61.5% ± 5.1% by PIT with 50 and 30 J/cm², respectively. A431 tumors irradiated with only 10 J/cm² showed no significant shortening of FLT immediately after PIT. FLT shortened by only 7.7% at 48 hours after PIT compared with the untreated control (Fig. 4A). Interestingly, the FLT of nonirradiated tumors in PIT treated mice shortened slightly more than that in the untreated mice, but these changes were not significant, however, FLT became shorter with larger doses of NIR light to the treated tumors. These changes may be caused small amounts of light diffusing through the soft tissues from the "treated" side to the "untreated" side, thus explaining the dose-dependence of the effect.

Histologic analysis

Microscopy of treated tumors revealed various degrees of necrosis and microhemorrhage with clusters of healthy or damaged but potentially viable tumor cells after PIT. Necrotic damage was diffuse and intense and the amount of surviving tumor cells was reduced when 30 or 50 J/cm² of NIR light was administered. In contrast, when 10 J/cm² of NIR light was administered, necrotic cell damage was found in only limited areas with relatively large areas of viable cancer cells accounting for the majority of the tissue (Fig. 4C).

Discussion

Fluorescence microscopy studies showed Pan-IR700 gradually internalized into lysosomes in A431 cells at 37°C (Fig. 2). As Pan-IR700 internalized (Fig. 1D), IR700 FLT became longer as a function of incubation time. IR700 eventually accumulated in the lysosome. After exposure to a threshold intensity of NIR light, Pan-IR700 induced immediate outer cell membrane damage and damage to lysosomes, resulting in accumulation of IR700 within the cytoplasm and into the extracellular space. This damage was associated with a significant reduction in IR700 FLT. This implies that cellular internalization of the Pan-IR700 conjugate by itself prolongs IR700 FLT as it accumulates in the endolysosome. However, by damaging membrane structures, including the lysosomal membrane, PIT induces cell death and releases long FLT IR700, into the cytoplasm whereupon the FLT markedly shortens. Therefore, shortening FLT serves as an indicator of acute membrane damage induced by PIT.

Treatment with PIT with effective therapeutic light dose of NIR leads to shortened IR700 FLT in cancer cells *in vitro* and in tumors *in vivo*. The shortening of FLT was dependent on the dose of NIR light exposure *in vitro* (Fig. 1C). PIT with suboptimal doses of NIR light (10 J/cm²) did not show significant shortening of IR700 FLT *in vivo*. These differences could be

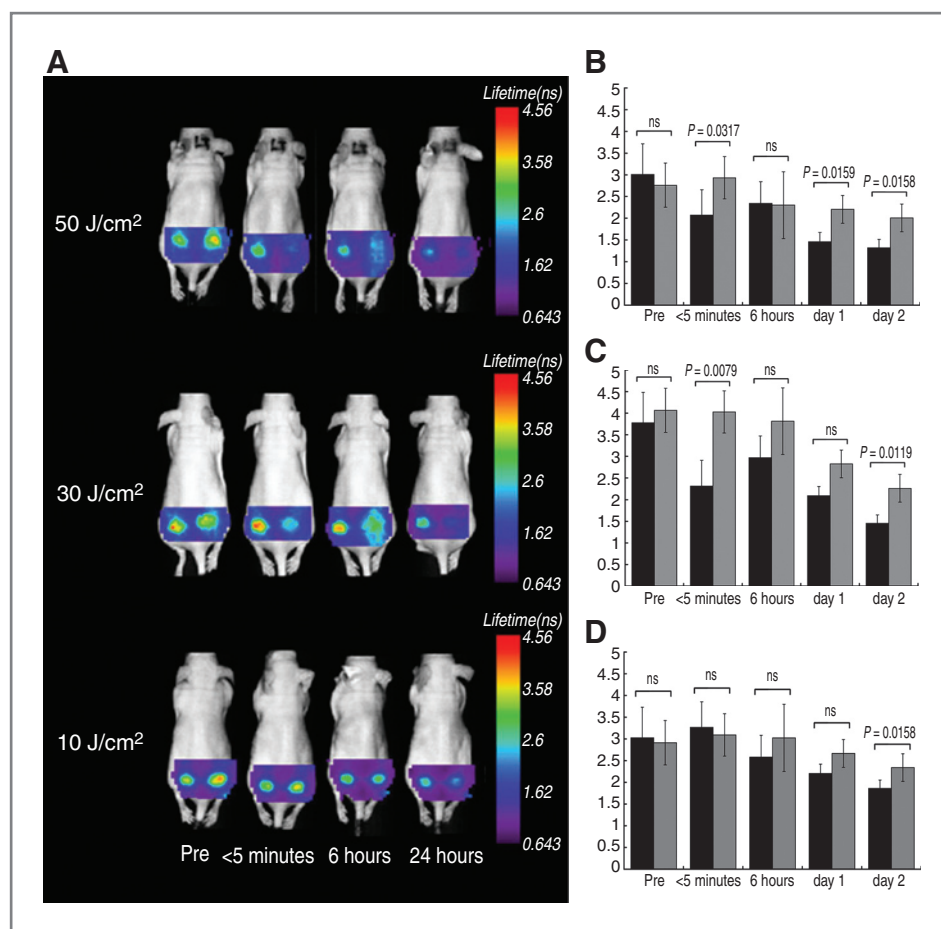


Figure 3. Comparison with FLT of irradiated tumors (dark gray bar) and nonirradiated tumors (bright gray bar). A, FLT images before and after PIT at the dose of 10, 30, and 50 J/cm² in the same mouse that was inoculated with A431 cells on both sides of the mouse dorsum. Right-sided tumor was treated by PIT, whereas the left was covered. FLT of A431 tumors treated with PIT with 50 J/cm² (B), 30 J/cm² (C), and 10 J/cm² (D) were plotted. PIT with the NIR light dose of 30 and 50 J/cm² showed significant ($P < 0.05$) shortenings in FLT immediately, compared with nonirradiated tumors. However, FLT did not significantly shorten at a low dose of 10 J/cm². Transient prolongations of FLT were observed at 6 hours after PIT likely due to uptake by reactive macrophages. Mann-Whitney's *U* test was used for the statistical analysis.

ascribed to the population of cancer cells, which received PIT effects. Our previous study showed that PIT with 50 J/cm² of NIR light exposure or more could eradicate A431 tumors. PIT with 30 J/cm² was not sufficient to totally eradicate tumors but caused tumor shrinkage and growth delay, indicating while not all cells were killed, most were severely and irreversibly damaged (2).

Shortened FLT of treated tumor *in vivo* was observed within 30 minutes of a single effective dose of NIR light and indicated a biologic effect several days before tumor size and shape changed. Although size of the lesion is considered a major indicator of cell death, it does not happen fast enough to determine if treatment has been effective. In the specific case of PIT, where light can be reapplied if necessary, a more immediate readout of cell death is needed. Size changes do not occur rapidly enough for monitoring cytotoxic effects. This is especially true of surgical or endoscopic procedures where it is preferable to complete treatments at one setting (2). FLT, because it is an immediate readout of the tumor's condition, can assess the therapeutic effects of PIT to the cancer cells immediately after treatment and aids in deciding whether additional doses of NIR light exposure are necessary or not during the procedure (15, 16).

Interestingly, after an initial shortening of the FLT, it briefly became longer at about 6 hours after PIT. By 24 hours after PIT the FLT was reduced again (Fig. 3). Since we have observed prolongation of IR700 FLT as it is being internalized we hypothesize that after cell membrane disruption caused by PIT, the IR700 leaks into the extracellular space where it is internalized by macrophages mobilized to respond to the release of cytokines associated with cell necrosis. This is supported by histologic findings at 6 hours post-PIT that show inflammatory infiltrates composed of macrophages, which are entering the space formerly occupied by viable tumor (1). This transient prolongation of IR700 FLT may therefore be a sign of effective cell damage followed by initiating tissue repair possibly mediated by the chemokine release or the toll-like receptor system induced by the fragmented DNA and lipid bilayer (17–19).

Fluorescent proteins (FP) are a potential alternative for monitoring tumor growth *in vivo* (20–23). Fluorescence imaging using FPs is better suited for longitudinal monitoring of the effects of photo-therapy (24, 25). Acutely, FPs retain their signal regardless of the viability of the cells and even in necrotic cells may be taken up by macrophages. Thus, even though FLT requires postprocessing of the fluorescence signal and uses relatively expensive equipment, it is better suited for detecting

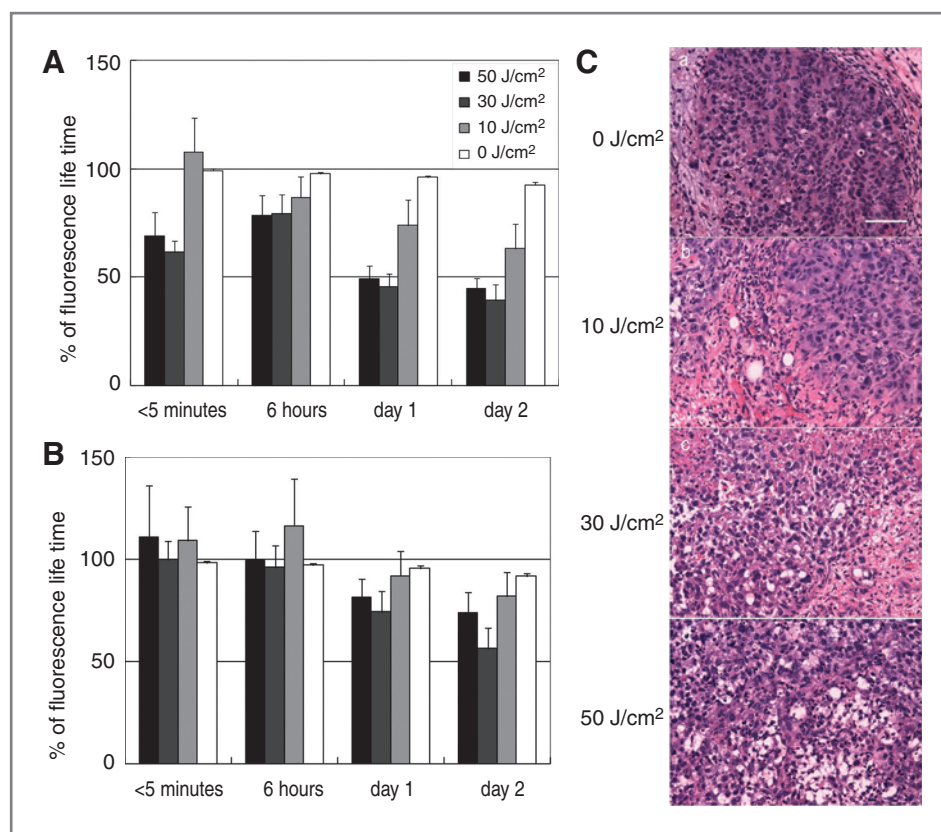


Figure 4. A, FLTI in PIT treated tumors with 50 and 30 J/cm² shortened significantly ($P < 0.01$) compared with no treatment control (0 J/cm², control). FLTIs were immediately shortened to $69.1 \pm 10.9\%$ and $61.5 \pm 5.1\%$ by PIT with 50 and 30 J/cm², respectively. A431 tumors irradiated with only 10 J/cm² showed no significant shortens of FLT that were seen immediately. FLT shortened by only 7.7% at 48 hours after PIT compared with no treatment control. B, FLT of nonirradiated tumors in PIT treated mice shortened slightly more than that in the untreated mice over time, but these changes were not significant. They may be caused by a small amount of light diffusing through tissue from the irradiated side, even though the surface of the tumor was covered. Student *t* test was used for the statistical analysis. C, histologic specimens of A431 tumors, which were treated with PIT at 0, 10, 30, and 50 J/cm², are shown. All specimens were stained with hematoxylin and eosin. Microscopic evaluation of treated tumors revealed various degrees of necrosis and microhemorrhage with clusters of healthy or damaged tumor cells after PIT. Necrotic damage was diffuse and intense and fewer surviving tumor cells were seen when 30 and 50 J/cm² of NIR light was administered. In contrast, when only 10 J/cm² of NIR light was administered, necrotic cell damage was found in only limited areas within the tumor while substantial amounts of healthy cancer foci remained. Scale, 50 μ m.

acute changes than FPs (26, 27). Fluorescence imaging with FPs has been used for longitudinal monitoring of the therapeutic effects of PIT (2). However, PIT-induced acute cell death can only be detected with optical methods such as FLTI while longer term changes can be measured with FPs. It should be noted, however, that FLTI is potentially clinically translatable while FPs, which require cell transfection are unlikely to be used clinically.

This data suggests that the FLTI of Pan-IR700 is a robust measurement that does not depend on the concentration of Pan-IR700 or light exposure in solution. For example, the *in vitro* Pan-IR700 solution did not change its FLTI at varying concentrations or after NIR light exposure with various doses. Therefore, only the surrounding chemical microenvironment seems to affect the IR700 FLTI. While IR700 is normally fluorescent and reflects tumor burden, after catabolism in the lysosome and photo-bleaching, fluorescence may be reduced, thus leading to ambiguity regarding tissue viability. However, those photo-chemical and biochemical changes do not affect

FLTI. Therefore, shortening of FLTI is a better biomarker than IR700 fluorescence intensity.

In conclusion, FLTI is a potential method of assessing in near real-time, the cytotoxic effects of PIT using a mAb-IR700 conjugate, during surgical or endoscopic procedures. FLTI is prolonged during endolysosomal internalization but rapidly shortened after cell damage. FLTI again is prolonged for a brief period about 6 hours after PIT due to internalization by migrating macrophages. After that there is a steady reduction in FLTI. Thus, FLTI imaging allows the assessment of the effect of PIT before morphologic changes become evident.

Disclosure of Potential Conflicts of Interest

No potential conflicts of interest were disclosed.

Authors' Contributions

Conception and design: P.L. Choyke, H. Kobayashi

Development of methodology: T. Nakajima, H. Kobayashi

Acquisition of data (provided animals, acquired and managed patients, provided facilities, etc.): T. Nakajima, K. Sano, M. Mitsunaga, H. Kobayashi

Analysis and interpretation of data (e.g., statistical analysis, biostatistics, computational analysis): T. Nakajima, K. Sano, M. Mitsunaga, P.L. Choyke, H. Kobayashi

Writing, review, and/or revision of the manuscript: T. Nakajima, P.L. Choyke, H. Kobayashi

Administrative, technical, or material support (i.e., reporting or organizing data, constructing databases): H. Kobayashi

Study supervision: H. Kobayashi

Grant Support

This research was supported by the Intramural Research Program of the National Institutes of Health, National Cancer Institute, Center for Cancer Research.

Received April 10, 2012; revised June 22, 2012; accepted July 9, 2012; published OnlineFirst July 16, 2012.

References

- Mitsunaga M, Ogawa M, Kosaka N, Rosenblum LT, Choyke PL, Kobayashi H. Cancer cell-selective *in vivo* near infrared photoimmunotherapy targeting specific membrane molecules. *Nat Med* 2011;17:1685–91.
- Mitsunaga M, Nakajima T, Sano K, Choyke PL, Kobayashi H. Near infrared theranostic photoimmunotherapy (PIT): repeated exposure of light enhances the effect of immunconjugate. *Bioconjug Chem* 2012;23:604–9.
- Mitsunaga M, Nakajima T, Sano K, Kramer-Marek G, Choyke PL, Kobayashi H. Immediate *in vivo* target-specific cancer cell death after near infrared photoimmunotherapy. *BMC Cancer* 2012;12:345. [Epub ahead of print]
- Young MR, Ileva LV, Bernardo M, Riffle LA, Jones YL, Kim YS, et al. Monitoring of tumor promotion and progression in a mouse model of inflammation-induced colon cancer with magnetic resonance colonography. *Neoplasia* 2009;11:237–46.
- Kosaka N, Ogawa M, Choyke PL, Kobayashi H. Clinical implications of near-infrared fluorescence imaging in cancer. *Future Oncol* 2009;5:1501–11.
- Hassan M, Riley J, Chernomordik V, Smith P, Pursley R, Lee SB, et al. Fluorescence lifetime imaging system for *in vivo* studies. *Mol Imaging* 2007;6:229–36.
- Berezin MY, Achilefu S. Fluorescence lifetime measurements and biological imaging. *Chem Rev* 2010;110:2641–84.
- Clegg RM, Holub O, Gohlke C. Fluorescence lifetime-resolved imaging: measuring lifetimes in an image. *Meth Enzymol* 2003;360:509–42.
- Han S-H, Farshchi-Heydari S, Hall DJ. Analysis of the fluorescence temporal point-spread function in a turbid medium and its application to optical imaging. *J Biomed Opt* 2008;13:064038.
- Alford R, Ogawa M, Hassan M, Gandjbakhche AH, Choyke PL, Kobayashi H. Fluorescence lifetime imaging of activatable target specific molecular probes. *Contrast Media Mol Imaging* 2010;5:1–8.
- Keren S, Gheysens O, Levin CS, Gambhir SS. A comparison between a time domain and continuous wave small animal optical imaging system. *IEEE T Med Imaging* 2008;27:58–63.
- Bloch S, Lesage F, McIntosh L, Gandjbakhche A, Liang K, Achilefu S. Whole-body fluorescence lifetime imaging of a tumor-targeted near-infrared molecular probe in mice. *J Biomed Opt* 2005;10:054003.
- Hutchinson CL, Lakowicz JR, Sevick-Muraca EM. Fluorescence lifetime-based sensing in tissues: a computational study. *Biophys J* 1995;68:1574–82.
- Ma G, Gallant P, McIntosh L. Sensitivity characterization of a time-domain fluorescence imager: eXplore Optix. *Appl Opt* 2007;46:1650–7.
- Kosaka N, Mitsunaga M, Longmire MR, Choyke PL, Kobayashi H. Near infrared fluorescence-guided real-time endoscopic detection of peritoneal ovarian cancer nodules using intravenously injected indocyanine green. *Int J Cancer* 2011;129:1671–7.
- Longmire M, Kosaka N, Ogawa M, Choyke PL, Kobayashi H. Multicolor *in vivo* targeted imaging to guide real-time surgery of HER2-positive micrometastases in a two-tumor coincident model of ovarian cancer. *Cancer Sci* 2009;100:1099–104.
- Emeagi PU, Van Lint S, Goyvaerts C, Maenhout S, Cauwels A, McNeish IA, et al. Proinflammatory characteristics of SMAC/DIA-BLO-induced cell death in antitumor therapy. *Cancer Res* 2012;72:1342–52.
- Shiratsuchi A, Watanabe I, Takeuchi O, Akira S, Nakanishi Y. Inhibitory effect of toll-like receptor 4 on fusion between phagosomes and endosomes/lysosomes in macrophages. *J Immunol* 2004;172:2039–47.
- Zhu P, Baek SH, Bourk EM, Ohgi KA, Garcia-Bassets I, Sanjo H, et al. Macrophage/cancer cell interactions mediate hormone resistance by a nuclear receptor derepression pathway. *Cell* 2006;124:615–29.
- Kimura H, Lee C, Hayashi K, Yamauchi K, Yamamoto N, Tsuchiya H, et al. UV light killing efficacy of fluorescent protein-expressing cancer cells *in vitro* and *in vivo*. *J Cell Biochem* 2010;110:1439–46.
- Tsai MH, Aki R, Amoh Y, Hoffman RM, Katsuoka K, Kimura H, et al. GFP-fluorescence-guided UVC irradiation inhibits melanoma growth and angiogenesis in nude mice. *Anticancer Res* 2010;30:3291–4.
- Yamamoto N, Jiang P, Yang M, Xu M, Yamauchi K, Tsuchiya H, et al. Cellular dynamics visualized in live cells *in vitro* and *in vivo* by differential dual-color nuclear-cytoplasmic fluorescent-protein expression. *Cancer Res* 2004;64:4251–6.
- Hoffman RM, Yang M. Whole-body imaging with fluorescent proteins. *Nat Protoc* 2006;1:1429–38.
- Jiang P, Yamauchi K, Yang M, Tsuji K, Xu M, Maitra A, et al. Tumor cells genetically labeled with GFP in the nucleus and RFP in the cytoplasm for imaging cellular dynamics. *Cell Cycle* 2006;5:1198–201.
- Hoffman RM, Yang M. Subcellular imaging in the live mouse. *Nat Protoc* 2006;1:775–82.
- Hoffman RM, Yang M. Color-coded fluorescence imaging of tumor-host interactions. *Nat Protoc* 2006;1:928–35.
- Hoffman RM. The multiple uses of fluorescent proteins to visualize cancer *in vivo*. *Nat Rev Cancer* 2005;5:796–806.

Cancer Research

The Journal of Cancer Research (1916–1930) | The American Journal of Cancer (1931–1940)

Real-time Monitoring of *In Vivo* Acute Necrotic Cancer Cell Death Induced by Near Infrared Photoimmunotherapy Using Fluorescence Lifetime Imaging

Takahito Nakajima, Kohei Sano, Makoto Mitsunaga, et al.

Cancer Res 2012;72:4622-4628. Published OnlineFirst July 16, 2012.

Updated version Access the most recent version of this article at:
doi:[10.1158/0008-5472.CAN-12-1298](https://doi.org/10.1158/0008-5472.CAN-12-1298)

Supplementary Material Access the most recent supplemental material at:
<http://cancerres.aacrjournals.org/content/suppl/2012/09/12/0008-5472.CAN-12-1298.DC1>

Cited articles This article cites 26 articles, 4 of which you can access for free at:
<http://cancerres.aacrjournals.org/content/72/18/4622.full#ref-list-1>

Citing articles This article has been cited by 2 HighWire-hosted articles. Access the articles at:
<http://cancerres.aacrjournals.org/content/72/18/4622.full#related-urls>

E-mail alerts [Sign up to receive free email-alerts](#) related to this article or journal.

Reprints and Subscriptions To order reprints of this article or to subscribe to the journal, contact the AACR Publications Department at pubs@aacr.org.

Permissions To request permission to re-use all or part of this article, use this link
<http://cancerres.aacrjournals.org/content/72/18/4622>.
Click on "Request Permissions" which will take you to the Copyright Clearance Center's (CCC) Rightslink site.